16th World Conference on Earthquake, 16WCEE 2017

Santiago Chile, January 9th to 13th 2017

Paper N° 2918 (Abstract ID)

Registration Code: S-Z1463198223

# EXPERIMENTAL STUDY ON SHEAR BEHAVIOR OF EXTERIOR STEEL BEAM TO REINFORCED CONCRETE COLUMN JOINTS

A. Kitano[(1)], N. Baba[(2)]

[(1)] *Associate Professor, Maebashi Institute of Technology, kitano@maebashi-it.ac.jp*
[(2)] *Associate Professor, Osaka Institute of Technology, nozomu.baba@oit.ac.jp*

## *Abstract*

There is the popularity on the steel beam to reinforced concrete (RC) columns structure which mechanically placed in the right member in the right places. Though, the stress transfer mechanism of beam–column joint in this structure has been clarified only interior beam–column joint. Therefore, there are no design guidelines of this structure in Japan. There has been much research on interior beam–column joints in which the steel beams are continuous through the RC columns. In contrast, few experiments have been carried out on exterior beam–column joints, which, like the steel beams, are embedded in the RC columns. Therefore, in the present paper we perform experiments to elucidate the shear behavior of an exterior beam–column joint of a steel-beam-to-RC-column structure. The purpose of this study is to examine the stress transfer mechanism given that the embedded length of the steel beam is at most 70% of the RC column depth. We also examine through experiment how the ratio of steel beam width to RC column width and the ratio of steel beam embedded length to RC column depth affect the bearing stress, which is one of the measures of beam–column joint ultimate strength. The specimen configuration involves one beam and two column segments between the inflection points in a frame subjected to lateral loading. The contraction scale of the test specimens was approximately half of a steel beam to RC column structure, assuming the presence of an exterior beam–column joint in the middle floor in a multi-storey multi-span building. The specimens were loaded with a lateral cyclic shear force by a jack at the top of the steel beam. The results show that although the depth of the RC column had no effect on RC column strength, when the steel embedded length was same length, the width of the RC column did influence the its strength. The beam–column joint had two failure modes: bearing failure and raking-out failure. The latter was a more brittle failure mode than the former. The failure mode and deformation capacity depended on the embedded length of the steel beam in the RC column. The raking-out failure occurred in the concrete in the tension side of the steel embedded part, when the embedded length was less than half of the RC column depth. The raking-out failure strength could be predicted theoretically according to the Architectural Institute of Japan Reinforced Concrete guideline, but the ultimate strength was almost equivalent to the bearing failure strength.

*Keywords: steel beam to RC column structure; beam–column joint; bearing stress; raking-out failure; embedded length*

## 1. Introduction

There is the popularity on the steel beam to reinforced concrete (RC) columns structure which mechanically placed in the right member in the right places. There has been much research on interior beam–column joints in which the steel beams are continuous through the reinforced concrete (RC) columns. In contrast, few experiments have been carried out on exterior beam–column joints, which, like the steel beams, are embedded in the RC columns. Therefore, in the present paper we perform experiments to elucidate the shear behavior of an exterior beam–column joint of a steel-beam-to-RC-column structure.

The purpose of this study is to examine the stress transfer mechanism given that the embedded length of the steel beam is at most 70% of the RC column depth. We also examine through experiment how the ratio of steel beam width to RC column width and the ratio of steel beam embedded length to RC column depth affect the bearing stress, which is one of the measures of beam–column joint ultimate strength.

## 2. Resistance Mechanism of Beam–column Joint

At present, when connecting a steel beam to an RC column structure, the shear resistance mechanism and the evaluation method are only proposed on the interior beam–column joint in which the steel beam is continuous through the RC column [1]. However, the exterior beam–column joint also appears to be able to provide a resistance mechanism and evaluation method akin to those of the interior beam–column joint. The bearing resistance mechanism in the exterior beam–column joint, of which the embedded length of the steel beam in the RC column is small, is shown in Fig. 1(a) to (c). The beam–column joint is composed inside component which

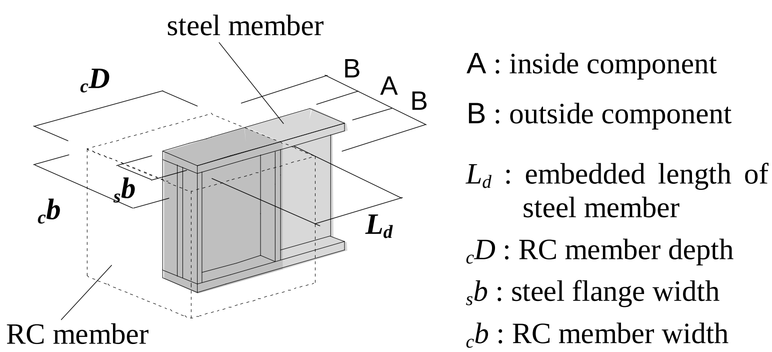


(a) Composition of exterior beam–column joint

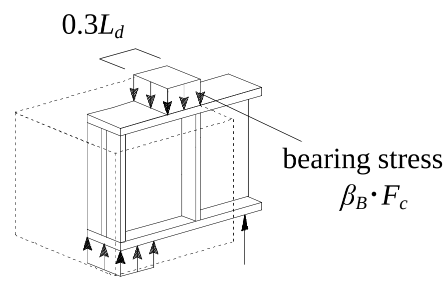


(b) Bearing mechanism

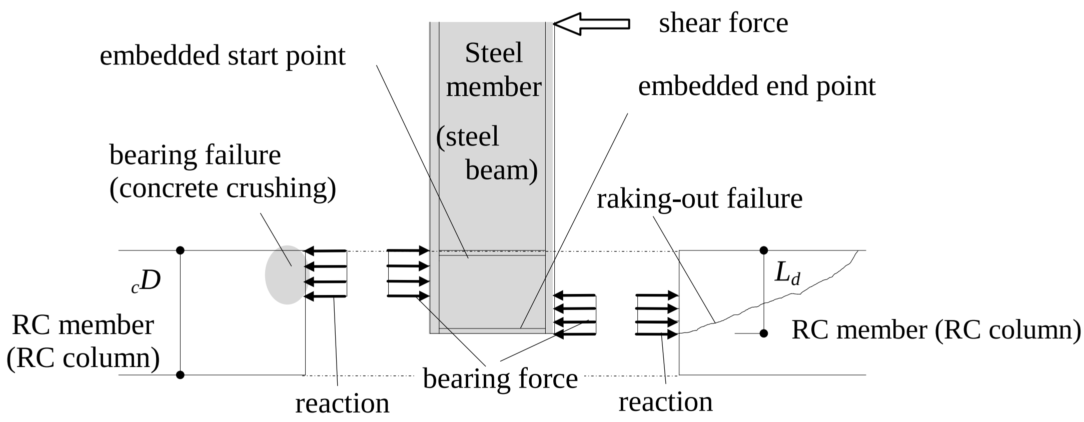


(c) Resistance mechanism and failure mode with bearing force (free body diagram)

Fig. 1 – Resistance mechanism of an exterior beam–column joint in which the embedded length of the steel member is shorter than the RC member depth

surrounded in steel flange width and outside component which except for it. It is possible to evaluate the ultimate strength of a beam–column joint by the summation of the strength of the inside and outside components. When the embedded length of the steel member is small, the concrete appears to collapse under a bearing force, which affects the interior beam–column joint and the steel flange plane in the side of the steel member containing the embedded starting point. Furthermore, the bearing force acting on the steel flange plane can cause the embedded end point of the steel member to extend further into the concrete, which results in punching shear failure of the concrete. This failure mode produces destruction equal to that of raking-out failure of the beam main bar in the RC exterior beam–column joint. Therefore, in this study, the failure mode was defined as raking-out failure by the steel bearing force, and bearing failure and raking-out failure occurred on the inside component of the beam–column joint.

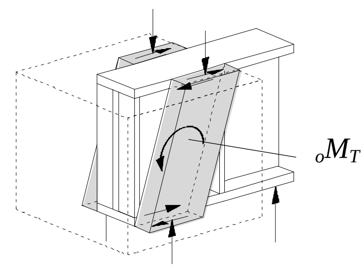


$_oM_T$ : torsional moment

Fig. 2 – Shear resistance mechanism of outside component

The shear resistance mechanism of the outside component of the beam–column joint is shown in Fig. 2. The torsional moment between the inside and outside components is resisted by the shear strength of the outside component [2]. In this study we produced specimens in which the torsional moments of the inside and outside components were removed, and evaluated the strength of the inside component of the beam–column joint in which the embedded length of the steel member was smaller than the RC column depth.

## 3. Experimental Procedure

### 3.1 Test specimens and materials

The experiment was divided into two series. Series 1 examined how steel embedded depth and RC column width affected beam–column joint failure, and likewise series 2 examined the roles of RC column depth, the strength of the inside component of the beam–column joint and its torsional moment. The dimensions and details of the

Table 1 – Details of specimens

| specimen | | RC column width $_cb$ (mm) | RC column depth $_cD$ (mm) | Steel beam embedded length $L_d$ (mm) | $\xi$ $L_d/_cD$ | note |
|---|---|---|---|---|---|---|
| Series 1 | No. 1 | 300 | 300 | 200 | 0.67 | |
| | No. 2 | 300 | 300 | 150 | 0.50 | |
| | No. 3 | 500 | 300 | 150 | 0.50 | |
| Series 2 | No. 4 | 300 | 300 | 200 | 0.67 | |
| | No. 5 | 300 | 450 | 200 | 0.44 | |
| | No. 6 | 300 | 300 | 200 | 0.67 | torsional moment insulation |
| | No. 7 | 300 | 450 | 200 | 0.44 | torsional moment insulation |
| | No. 8 | 500 | 300 | 200 | 0.67 | torsional moment insulation |
| | No. 9 | 300 | 300 | 150 | 0.50 | bearing stress insulation |
| | No. 10 | 500 | 300 | 150 | 0.50 | bearing stress insulation |

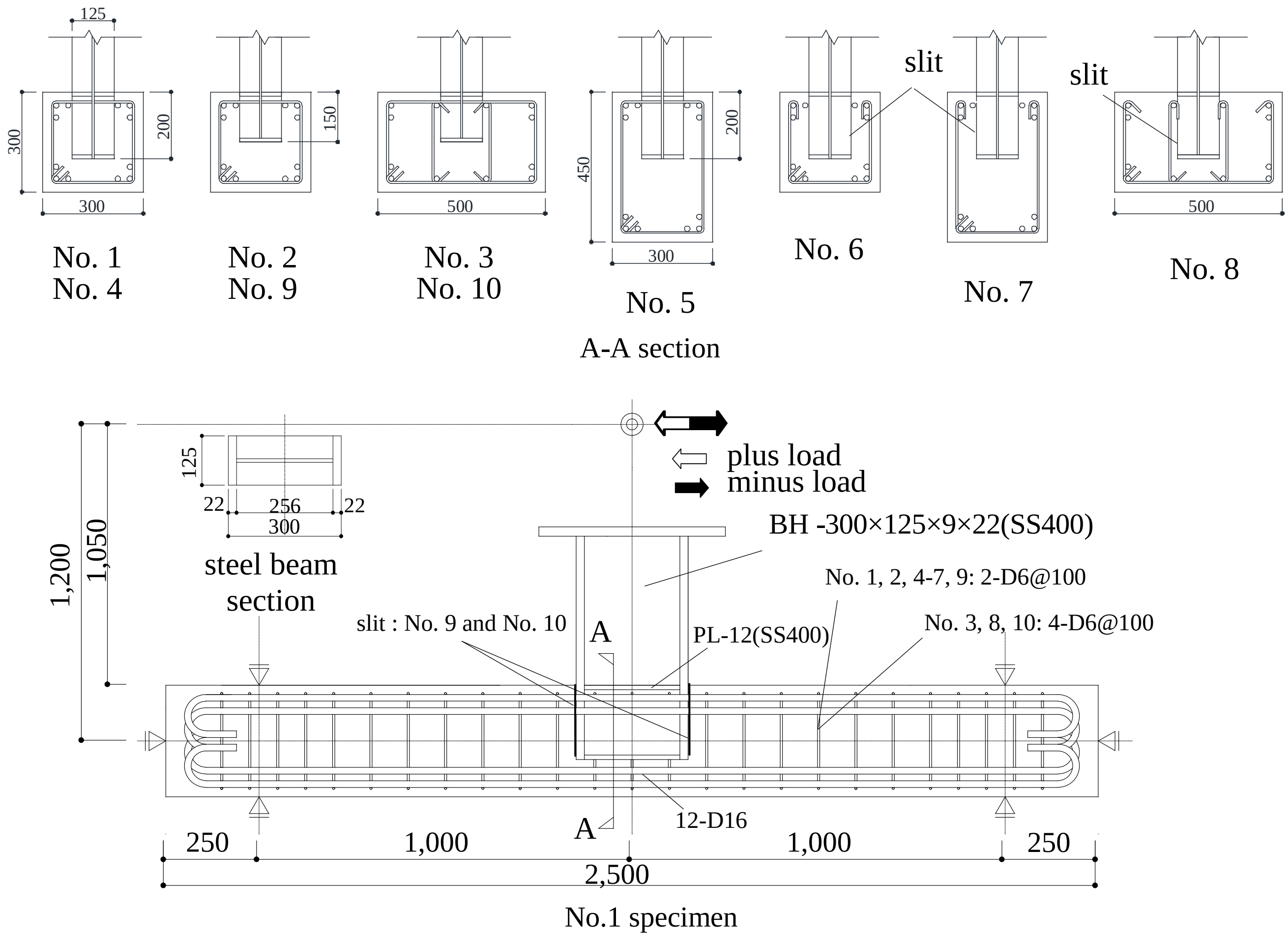


Fig. 3 – Details of specimens

test specimens are given in Fig. 3 and Table 1. The specimen configuration involves one beam and two column segments between the inflection points in a frame subjected to lateral loading. The contraction scale of the test specimens was approximately half of a steel beam to RC column structure, assuming the presence of an exterior beam–column joint in the middle floor in a multi-storey multi-span building. To ensure that beam–column joint failure occurs before any other failure, the beam–column joint strength was designed to be smaller than the flexural and shear strengths of the beam and column. Moreover, the bearing strength was designed to be smaller than the shear strength, which was calculated according to the method specified by the Architectural Institute of Japan [1]. The variables of the experiment were cross-sectional shape of the RC column and embedded length of the steel beam in the RC column. Four cross-sectional shapes of the RC column (${}_cb \times {}_cD$) were trialed: 300×300, 300×400, 300×450 and 500×300 mm. Likewise, there were two values for the embedded length of the steel beam: 150 mm and 200 mm. The cross-sectional shape of the steel beam was made to be BH-300×125×9×22. Specimens No. 1–5 were ordinary specimens. Among them, specimens No. 1 and No. 4 were the standard specimens for each series. Specimens No. 6–8 were made for the purpose of evaluating the strength of the inside component of the beam–column joint. These specimens left 1 mm clearance in the steel member embedding of the RC to remove stress transmission of the inside and outside components. Specimen No. 9 and No. 10 were made for the evaluation of the torsional moment between the inside and outside components. These specimens left 10 mm clearance between the steel flange and RC column to remove the bearing stress on the inside component.

The mechanical properties of the materials are shown in Tables 2 and 3. For all specimens the main column reinforcement bar was 12-D16 and the shear reinforcement bar was D6@100. The shear reinforcement

Table 2 – Mechanical properties of steels

| position and class | | specimen | yield stress $\sigma_y$ (N/mm$^2$) | yield strain $\varepsilon_y$ (N/mm$^2$) | Young's modulus $E$ (kN/mm$^2$) |
|---|---|---|---|---|---|
| RC column | column main bar D16 (SD295) | No. 1 - No. 3 | 359 | 1910 | 190 |
| | | No. 4 - No. 10 | 345 | 1885 | 183 |
| | shear reinforcement D6 (SD295) | No. 1 - No. 3 | 372 | 3770 | 210 |
| | | No. 4 - No. 10 | 360 | 3720 | 209 |
| steel beam | web PL-9 (SS400) | all specimens | 286 | 1543 | 185 |
| | stiffener PL-12 (SS400) | | 292 | 1560 | 187 |
| | flange PL-22 (SS400) | | 264 | 1505 | 176 |

Table 3 – Mechanical properties of concrete

| specimen | compressive stress $\sigma_B$(N/mm$^2$) | compressive strain $\varepsilon_U$(μ) | tensile stress $\sigma_t$(N/mm$^2$) | Young's modulus $E$(kN/mm$^2$) |
|---|---|---|---|---|
| No. 1 | 29.3 | 2140 | 2.94 | 22.2 |
| No. 2 and No. 3 | 31.7 | 2480 | 2.74 | 21.7 |
| No. 4 to No. 10 | 27.6 | 2230 | 1.98 | 20.0 |

of the beam–column joint was run through the hole in the steel web. However, on No.6–8 specimen which insulated torsional moment, the shear reinforcement of the beam–column joint was anchored to main reinforcement of the outside component.

### 3.2 Loading and instrumentation

The specimen was installed in the loading equipment so that the RC column was level and the steel beam was vertical. The specimens were loaded with a lateral cyclic shear force by a horizontal jack at the top of the steel beam. Both ends of the column were supported by the pin roller. Though this loading condition is different from the actual behavior of the structure in earthquake, the stress behavior of the beam–column joint becomes equal even in the load with the beam. The incremental loading cycles were controlled by the story drift angle, $R$, defined as the ratio of lateral displacement to beam length, $\delta/l$. The lateral load sequence consisted of two cycles for each story deformation angle, $R$: 0.002, 0.004, 0.010, 0.020, 0.030 and 0.040 radians.

## 4. Experimental Results and Discussion

### 4.1 Conditions for failure

The failure conditions of each specimen after testing are shown in Fig. 4. For all specimens, an initial bending crack in the RC column and shear crack in the beam–column joint appeared for $R$ = 0.002 to 0.004 radians. For specimens No. 1 and No. 4, numerous shear cracks appeared in the beam–column joint and concrete collapse occurred on the compression side of the steel flange at the embedded starting point. The story drift angle at maximum strength was approximately $R$ = 0.02 radians. After maximum strength was reached, the concrete on the compression side of the steel flange at the embedded starting point was being crushed at $R$ = 0.03 radians, causing bearing failure. In contrast, for specimen No. 5, although shear cracks appeared in the beam–column joint, concrete collapse was not observed. Furthermore, the diagonal crack on the tension side of the steel beam flange in the embedded starting point propagated in the direction of the RC column, which led to crocodile cracking. After this occurred, the maximum strength had been achieved. Afterwards, although the widening of the diagonal cracks in the beam–column joint and in the tension side of the steel beam flange became notable, no concrete collapse in the compression side of the steel beam flange was observed. Therefore, these cracks would appear to have resulted from the RC column extending under the action of the bearing stress, affecting the steel flange in the steel member embedded end point. In other words, it appears to be raking-out failure of the RC member of the tensile side of the steel beam in the steel beam axial direction. In these crack situations, when the embedded length of the steel member was 200 mm, the specimen with an RC column depth of 300 mm was failed with bearing failure, and the specimen with an RC column depth of 450 mm failed from raking out.

For specimens No. 2 and No. 3, in which the steel embedded length was 150 mm, the shear cracks in the beam–column joint appeared in the concrete section embedded with the steel member. There were significant splitting cracks in the embedded endpoint on the tension side of the steel beam flange caused by the steel member raking out. The number of diagonal cracks in the beam–column joint of specimen No. 3, in which the RC column was wide, was less than that of specimen No. 2 having equal steel embedded length. The diagonal

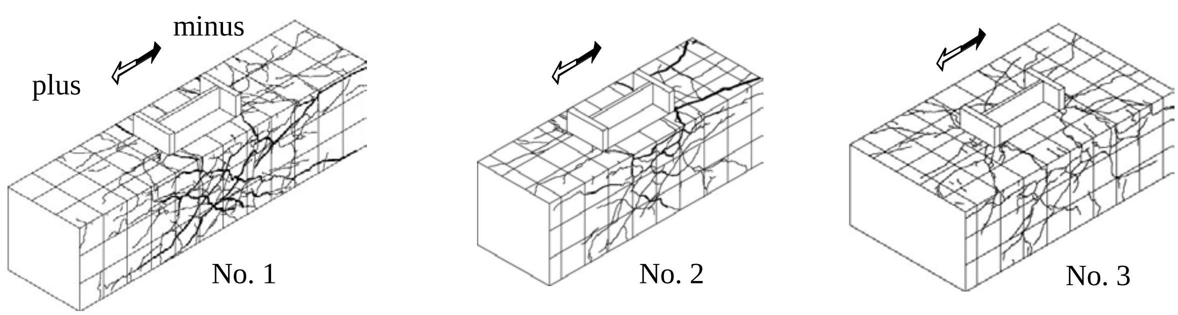


(a) Series 1

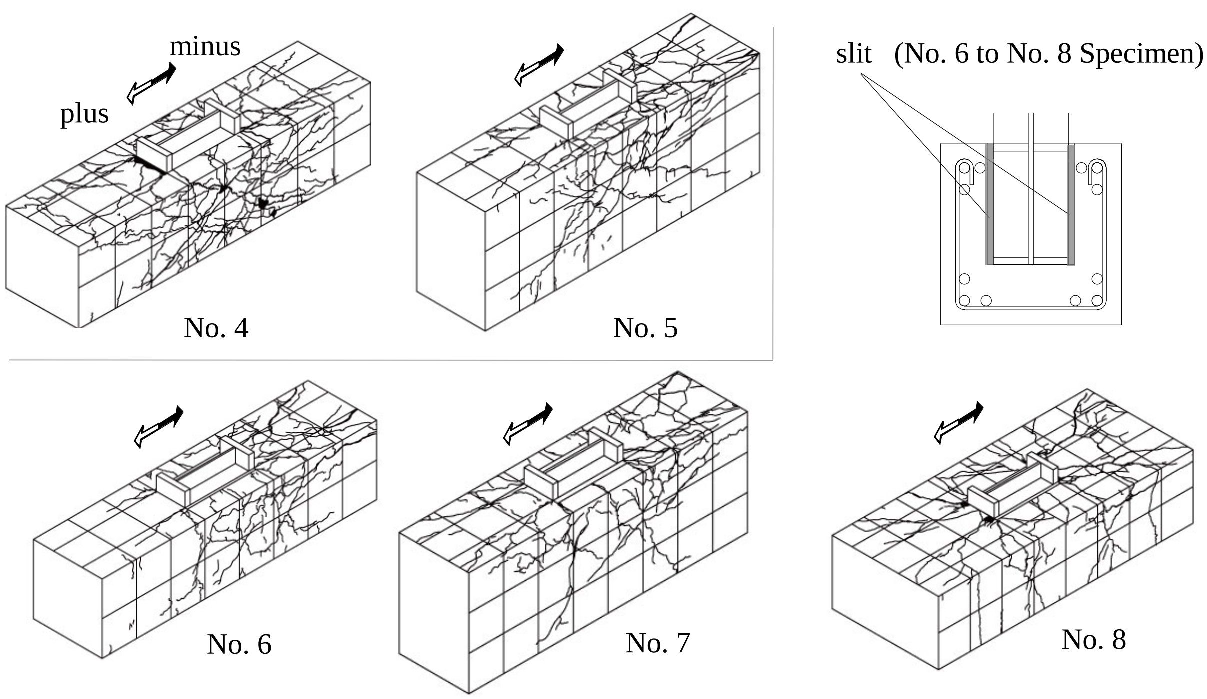


(b) Series 2

Fig. 4 – Failure condition

cracks and splitting cracks did not experience much propagation.

Specimens No. 6–8, which insulated interior component with the outside component, exhibited the same failure condition as specimen No. 5. Therefore, the failure mode of these specimens is designated as raking-out failure.

## 4.2 Load versus displacement relationship

The interaction curves of the column shear force $_{C}Q$ and story deformation angle $R$ for several specimens are shown in Figs. 5 and 7. From these plots the skeleton curves were derived, which are presented for comparison in Figs. 6 and 8.

In series 1, all specimens showed reverse sigmoid hysteresis of inferior energy absorption. Although maximum strength was achieved at $R$ = 0.02 radians/cycle in all specimens, regardless of the experimental variable, the reduction of the load after maximum strength was more dramatic for specimens No. 2 and 3, in which the steel embedded length was short, than for specimen No. 1. The influence of steel embedded length can be observed by comparing specimens No. 1 and 2 in Fig. 6; the maximum strength of specimen No. 1 was higher than that of specimen No. 2. Likewise, the effect of RC column width on maximum strength can be observed by comparing specimens No. 2 and 3 in the same figure. Specimen No. 3 with the widest RC column had the highest maximum strength.

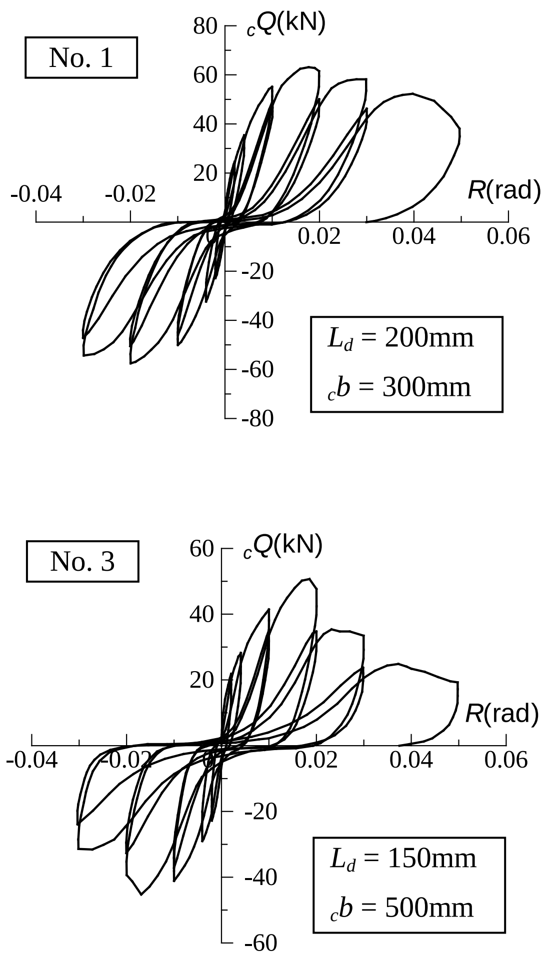


Fig. 5 – Interaction curves

(Series 1)

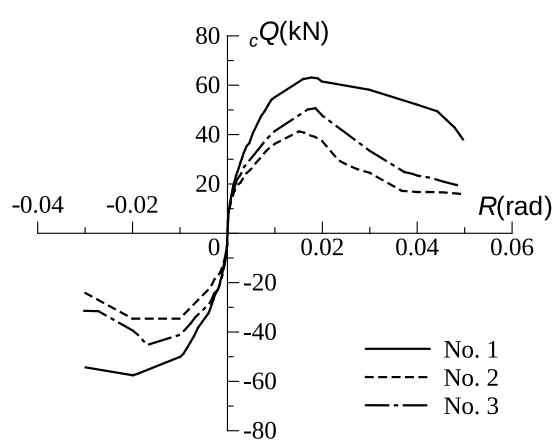


Fig. 6 – Comparison of skeleton curves

(Series 1)

In series 2, specimens No. 4 and 5 showed reverse sigmoid hysteresis from early on in the cyclic loading. Specimen No. 5 in which the RC column was deep exhibited a more pronounced pinching shape in the later loading cycles. Therefore, when the embedded length of the steel member of the RC column decreased, the energy absorption was inferior. And, the initial stiffness of specimen No. 5 was higher than specimen No. 4. As this reason, the stiffness of the RC column seems to affect it, since the RC column cross section of specimen No.

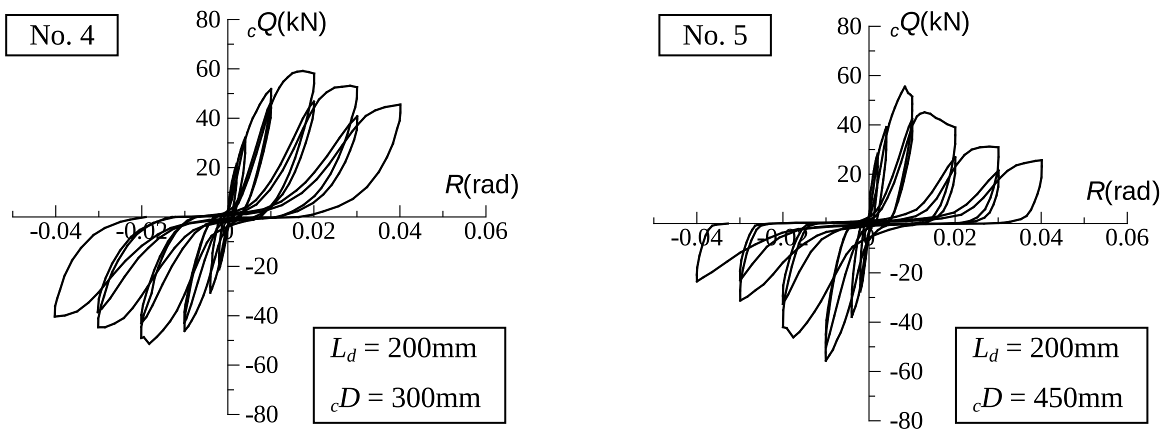


(a) normal specimen

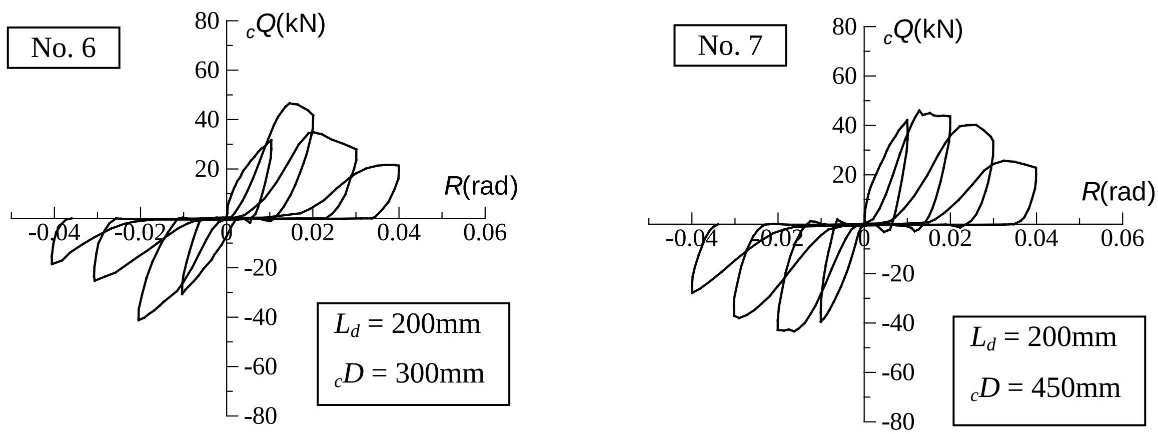


(b) torsional-moment-isolated specimen

Fig. 7 – Interaction curves (Series 2)

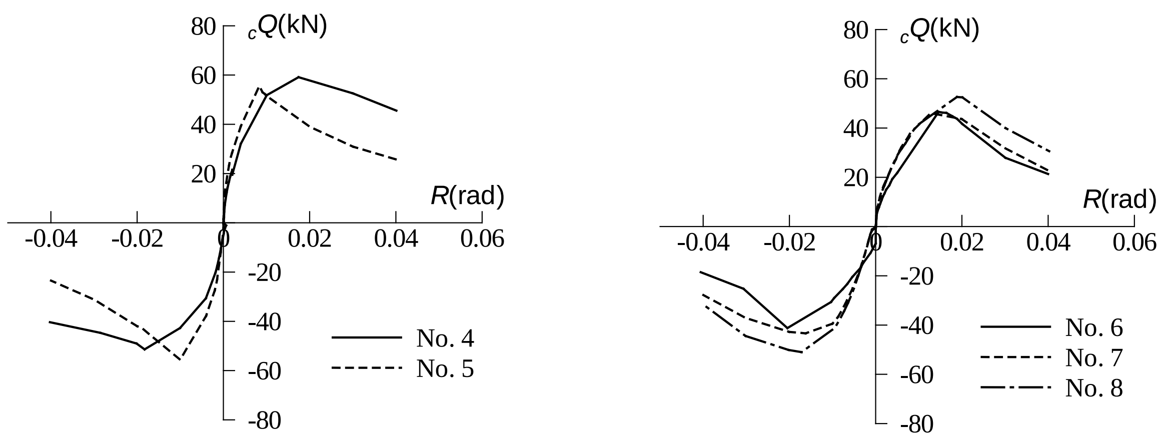


(a) normal specimen (b) torsional-moment-isolated specimen

Fig. 8 – Comparison of skeleton curves (Series 2)

5 is bigger than specimen No. 4. However, specimen No. 4 was higher for the maximum load and was also larger on displacement of that. As specimen No. 4 experienced bearing failure and specimen No. 5 raking-out failure, their displacements differed at maximum strength, as did their behavior after the loading to reach this state was reduced.

The effects of RC column width can be observed in Fig. 8 by comparing specimens No. 6 and 7, which isolated the inside component from the outside component. The initial stiffness of specimen No. 7 was larger than that of specimen No. 6, but at maximum load this difference was no longer observed, and the load reduction ratio after maximum strength was achieved was also almost same for both specimens. The maximum strength of specimen No. 8 in which the RC column was wide was higher than those of specimens No. 6 and 7 by approximately 10%. In contrast, the load reduction ratio following maximum strength was almost the same and the effect of RC column width on deformability was not observed. Therefore, the maximum strength seems to be evaluated by steel embedded length. The effective horizontal projection area of the raking out concrete component increases in proportion to the increase in RC column width, improving the maximum strength.

### 4.3 Evaluation of ultimate strength of beam–column joint

The experimental and calculated values of ultimate strength are shown in Table 4, with the salient formulae listed in Table 5. The strengths of beam–column joints were calculated with the RCS equation [1] and the raking-out (AIJ) equation [3]. In the RCS calculations, the RC column depth ${}_{C}D$ was replaced with the steel embedded length *Ld* because no significant damage was observed in RC, except in the steel embedding area in beam–column joint at failure. For specimens No. 6–8, in which the inside component was isolated from the outside component, the following strengths were disregarded: the torsion strength (RCS equation) and the shear reinforcement strength in the beam–column joint (AIJ equation).

The calculated strength of the beam–column joint (RCS equation) underestimated the experimental value by approximately 10% in specimens No. 2 and 3, in which the steel embedded length was half of the RC column depth. Conversely, in specimens that had a steel embedded length less than half of the RC column depth, the calculated strength overestimated the experimental value. Furthermore, in all specimens in which the inside component was isolated from the outside component; the calculated strength underestimated the experimental value. The AIJ equation was applied to the cases in which the embedded length of the beam in the exterior

Table 4 – Experimantal and caluculated values of ultimate strength

| specimen | | experimental values | calculated ultimate strength | | | | failure mode |
|---|---|---|---|---|---|---|---|
| | | maximum strength | RCS equation [1] | | AIJ equation [2] | | |
| | | ${}_{exp.C}Q$ (kN) | ${}_{cal1.C}Q$ (kN) | *exp./cal1* | ${}_{cal2.C}Q$ (kN) | *exp./cal2* | |
| Series 1 | No. 1 | 63.1 | 63.6 | 0.99 | 51.5 | 1.23 | bearing |
| | No. 2 | 41.3 | 38.9 | 1.06 | 40.5 | 1.02 | raiking-out |
| | No. 3 | 50.7 | 46.2 | 1.10 | 54.2 | 0.94 | raiking-out |
| Series 2 | No. 4 | 59.2 | 61.2 | 0.97 | 48.6 | 1.22 | bearing |
| | No. 5 | 55.6 | 66.2 | 0.84 | 52.3 | 1.06 | raiking-out |
| | No. 6 | 46.6 | 39.9 | 1.17 | 43.6 | 1.07 | bearing |
| | No. 7 | 46.1 | 30.2 | 1.52 | 46.9 | 0.98 | raiking-out |
| | No. 8 | 52.6 | 28.0 | 1.88 | 52.6 | 1.00 | raiking-out |
| | No. 9 | 16.9 | 16.6 | 1.02 | — | — | — |
| | No. 10 | 26.4 | 23.7 | 1.11 | — | — | — |

Table 5 – Strength calculation equations

<table>
<tr><td colspan="2">RCS equation [1]:</td></tr>
<tr><td>

$$ {}_pM_B = {}_iM_B + {}_oM_T $$

$$ {}_iM_B = 0.21\,{}_CD^2 \cdot {}_Sb \cdot \beta_B \cdot F_c $$

$$ {}_oM_T = \left(0.26 + 3.22\,{}_{Jw}p \cdot {}_w\sigma_Y \frac{{}_Cb}{{}_CD} \cdot \frac{1}{F_c}\right)\left\{\frac{{}_SD^2\left(3\,{}_CD - {}_SD\right)F_c}{6}\right\} + \frac{\mu_{fr} \cdot 0.3\,{}_CD \cdot {}_Sb \cdot \beta_B \cdot F_c \cdot {}_SD^2}{{}_rl} $$

In this study: ${}_oM_T$ was calculated by replacing ${}_CD$ with $L_d$

</td><td>

${}_pM_B$ : bearing strength<br>
${}_iM_B$ : bearing strength of inside component<br>
${}_oM_T$ : torsional moment between inside and outside components<br>
${}_CD$ : depth of RC member<br>
${}_SD$ : depth of steel member<br>
${}_Cb$ : width of RC member<br>
${}_Sb$ : width of steel member<br>
${}_{Jw}p$ : shear reinforcement ratio of beam–column joint<br>
$F_c$ : specified design strength of concrete<br>
$\mu_{fr}$ : friction coefficient (=0.211)<br>
$\beta_B$ : bearing effect coefficient (=1.5)<br>
${}_w\sigma_Y$ : yield stress of shear reinforcement bar

</td></tr>
<tr><td colspan="2">AIJ equation [3]:</td></tr>
<tr><td>

$$ T = k_n \cdot \left(T_c + T_w\right) $$

$$ T_c = \frac{2 \cdot l_{dh} \cdot b_e \cdot \sqrt{{l_{dh}}^2 + j^2}}{j} \cdot \sqrt{\sigma_B} $$

$$ T_w = 0.7 \cdot A_w \cdot \sigma_{wy} $$

$$ k_n = 1 + \sqrt{\frac{\sigma_0}{\sigma_B}} \quad \left(\text{where, } k_n \le 1 + 0.0016\sigma_B\right) $$

$$ b_e = b + C_{e1} + C_{e2} $$

In this study:<br>
- $T_c$ was calculated by replacing $l_{dh}$ with $L_{dh}$<br>
- $T$ was the steel flange tensile force<br>
- $b$ was the flange width

</td><td>

$T$ : strength of anchor bars<br>
$T_c$ : strength of burden share of concrete<br>
$T_w$ : strength of burden share of shear reinforcement bars<br>
$l_{dh}$ : length of anchor bars<br>
$j$ : stress center distance of beam<br>
$b_e$ : effective width of column<br>
$b$ : distance of outermost edge of beam main bars<br>
$C_{e1}$,$C_{e2}$ : thickness of cover concrete of beam main bar in column (under 0.8 ldh)<br>
$A_w$ : section area of shear reinforcement of effective range<br>
$\sigma_{wy}$ : shear reinforcement stress<br>
$\sigma_B$ : compression stress of concrete<br>
$\sigma_0$ : axial stress of column

</td></tr>
</table>

beam–column joint of the RC structure was half of the RC column depth. Therefore, only specimens No. 2, No. 3, No. 5 and No. 7 were examined. The calculated values correlate well with the experimental values for all specimens, particularly for specimens No. 2 and 5 in which raking-out failure occurred in the tension side of the concrete in the steel member. Therefore, the AIJ equation is appropriate when the steel embedded length is short. In each specimen, if the bearing stress and raking-out strength of the inside component are equal, then the strength calculated from the RCS and AIJ equations will be almost equal. It was shown that the torsional moment strength values calculated with the RCS equation were satisfyingly close to the experimental values.

In the torsional moment between the inside and outside components, the values calculated with the RCS equation accurately predicted the experimental values in specimens No. 9 and 10.

## 5. Conclusions

This experimental study was carried out to elucidate the stress transfer mechanism in the exterior beam–column joint of a steel beam RC column structure in which the embedded length of the steel beam is 70% or less of the RC column depth. We draw the following conclusions:

1) Although the depth of the RC column had no effect on the strength, when the steel embedded length was same length, the width of RC column did affect the strength.

2) The failure mode and deformation capacity depended on the embedded length of the steel beam in the RC column.

3) The beam–column joint experienced two failure modes: bearing failure and raking-out failure.

4) The raking-out failure occurred in the concrete in the tension side of the steel embedded part, when the embedded length was less than half of the RC column depth.

5) The raking-out failure mode was a more brittle failure than the bearing failure mode.

6) The ultimate strength at raking-out failure could be determined using the AIJ RC guideline, although it was almost equivalent to bearing failure strength.

## 6. Acknowledgements

The authors would like to thank the staff and the students of Osaka Institute of Technology and Maebashi Institute of Technology, Japan, for their assistance in the experimental work.

## 7. References

[1] Architectural Institute of Japan (2011): Stress transferring mechanism and resistance mechanism of steel-reinforced concrete joints *(in Japanese)*

[2] Yasushi N, Kohei H, Soichiro O, Shoko N (2013): Stress transferring mechanism and resistance mechanism on corner and exterior steel beam-reinforced concrete column joints. *Journal of Structural and Construction Engineering (Transactions of AIJ)*, **78** (688), 1167-1174 *(in Japanese)*

[3] Architectural Institute of Japan (1999): Design guideline for earthquake resistant reinforced concrete buildings based on inelastic displacement concept *(in Japanese)*